

A Generalized Nucleation Theory for Ice Crystalline

Maodong Li,^{*} Yupeng Huang,[†] Yijie Xia,[‡] Dechin Chen,^{*} Cheng Fan,[‡] Lijiang Yang,[†] Yi Qin Gao,[§] and Yi Isaac Yang[¶]
(Dated: April 11, 2024)

Despite the simplicity of the water molecule, the kinetics of ice nucleation under natural conditions can be complex. We investigated spontaneously grown ice nuclei using all-atom molecular dynamics simulations and found significant differences between the kinetics of ice formation through spontaneously formed and ideal nuclei. Since classical nucleation theory can only provide a good description of ice nucleation in ideal conditions, we propose a generalized nucleation theory that can better characterize the kinetics of ice crystal nucleation in general conditions. This study provides an explanation on why previous experimental and computational studies have yielded widely varying critical nucleation sizes.

Water, a seemingly simple substance, exhibits remarkable complexity with over eighteen distinct phases[1, 2]. When cooled at atmospheric pressure, water’s thermodynamic equilibrium state is hexagonal ice (ice I_h)[3], while cubic ice (ice I_c)[1, 3, 4] represents a metastable phase[5]. Experiments were performed conducted to obtain pure ice I_c [6–9], and only recently was defect-free ice I_c obtained [1]. Molecular dynamics (MD) simulations offer an atomic-level perspective on phase transitions, including nucleation processes[10–13]. In particular, enhanced sampling techniques[14] enabled the study of both homogeneous nucleation of pure ice I_c or pure ice I_h through these simulations[15, 16].

However, the well-known Ostwald’s step rule[17] assumes that ice first nucleates in the form of ice I_c and then transforms into ice I_h with a long relaxation time[18, 19], which hints that ice I_c is faster in kinetics. Classical nucleation theory (CNT) is widely used to describe the kinetics of homogeneous nucleation. The formation of a critical nucleus (N_c) requires overcoming a free-energy barrier[20–22], ΔG_c :

$$\Delta G_c = \frac{16\pi\gamma^3}{3\rho_s^2 |\Delta\mu|^2}, \quad (1)$$

where ρ_s is the density of the solid phase, $\Delta\mu$ is the chemical potential difference between the solid and the fluid phase at the temperature at which the cluster is critical, and γ is the surface free energy. When we assume a spherical shape for a defect-free cluster, N_c can

be estimated by[20, 23]:

$$N_c = \frac{32\pi\gamma^3}{3\rho_s^2 |\Delta\mu|^3}. \quad (2)$$

Critical ice nuclei are relatively small and short-living[19, 20], making them difficult to observe in experiments. N_c is a temperature-sensitive value and becomes infinity at the melting temperature T_m [20–22]. Therefore, many researchers have investigated supercooled water around the so-called “no man’s land” temperature region (230 K)[15, 19, 20, 22, 24, 25]. Surprisingly, the values of N_c obtained in different studies varied considerably, ranging from 100 to 600 (see Table S1 in SI). The uncertainty in the measured or calculated values of N_c suggests that CNT (Eq. (1-2)) is very rudimentary for describing the kinetics of ice nucleation in the natural state.

Here, we used all-atom MD simulations to study the difference in kinetics between ideal and spontaneously grown ice crystal nuclei (FIG. 1). In our previous work[16], we have successfully achieved reversible phase transitions[15] between water and ice using enhanced sampling[26–28] which allowed us to obtain all possible ice states in the simulation system. In this study, we developed modified collective variables (CVs) to effectively simulate the process of phase transition, allowing water molecules to grow into spherical ice clusters of an arbitrary size in MD simulations (see Chapter-S(II-IV) in supplementary material). Such spontaneously grown ice clusters inevitably contain internal defects, which we use to resemble ice nuclei through spontaneous formation. In this simulation study, we obtained thousands of ice crystal nuclei with different sizes and polymorphisms, from which we selected 454 ice nuclei of suitable sizes and classified them into I_c , I_{sd} , and I_h for kinetic studies. Simulation details are given in Chapter-S(V) of the supplementary material for details. For comparison, we also prepared a series of ideal spherical ice nuclei of different sizes and polymorphisms, which were cut from three ideal ice I_c , I_{sd} , and I_h crystals[20]. Sixty samples were cut from each crystal giving a total number of 180.

We performed forward flux sampling (FFS)[19, 29], aka “seeding”[23, 30] MD simulation, at 230K to study the kinetics of different ice nuclei and attempt to find the

^{*} Institute of Systems and Physical Biology, Shenzhen Bay Laboratory, Shenzhen 518132, China

[†] College of Chemistry and Molecular Engineering, Peking University, Beijing 100871, China

[‡] College of Chemistry and Molecular Engineering, Peking University, Beijing 100871, China; Institute of Systems and Physical Biology, Shenzhen Bay Laboratory, Shenzhen 518132, China

[§] gaoyq@pku.edu.cn; College of Chemistry and Molecular Engineering, Peking University, Beijing 100871, China; Institute of Systems and Physical Biology, Shenzhen Bay Laboratory, Shenzhen 518132, China

[¶] yangyi@szbl.ac.cn; Institute of Systems and Physical Biology, Shenzhen Bay Laboratory, Shenzhen 518132, China

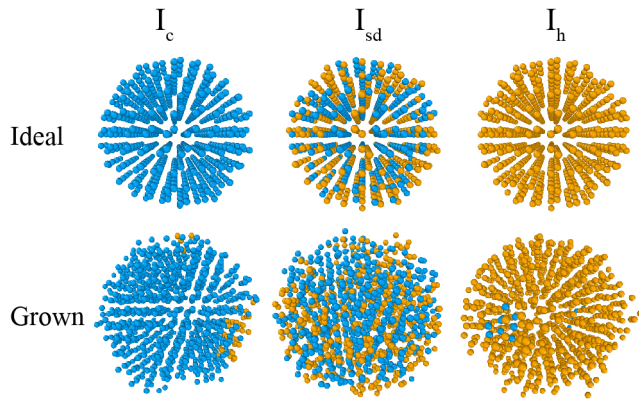


FIG. 1. Typical structures of ice nuclei. Each sphere represents an oxygen atom in a water molecule, where the blue and orange spheres represent water molecules in the cubic and hexagonal crystal states, respectively. (Upper) Ideal ice nuclei are cut spherically from perfect crystals. (Lower) Spontaneously grown ice nuclei nucleus by MD simulations.

size of the critical nuclei[19, 20]. We used the MD simulation software SPONGE[31] to perform “seeding” simulations for all 634 ice nuclei of at least 100 ns in a periodic box containing 23,040 all-atom TIP4P/Ice water molecule models. In order to eliminate the influence of liquid water around the ice clusters, we annealed each cluster for 1 ns before performing the simulations. See Chapter-S(IV) in the supplementary material for the simulation details. FIG. 2 shows the size change ΔN for different ice cluster size N at the end of the “seeding” simulation. We also employed other reaction coordinates (RCs) based on ΔN , such as $\Delta N/N$ and $N\%$ with details given in Chapter-S(VI) in the Supplementary Material. The “seeding” results indicate that CNT can describe well the kinetics of ideal ice nuclei. FIG. 2(a-c) shows that the variation of ΔN for the three ideal ice nuclei is in a positive linear relation with the ice cluster size. Therefore, we can easily determine their critical nucleus size N_c that fits the definition of CNT, i.e., the number of water molecules contained in the ice nucleus when $\Delta N = 0$. The N_c of the ideal ice nuclei of I_c , I_{sd} , and I_h all lie within a range of 255 to 295. For these perfect nuclei without defects, there does not seem to be much difference among different polymorphisms.

However, spontaneously grown ice nuclei possess kinetics that is obviously different from those of ideal nuclei. FIG. 2(d-f) reveals that while the ΔN of the grown nuclei generally increases with increasing ice cluster size, the data points are highly scattered and do not show a linear relationship as in the case of ideal nuclei. To further investigate the differences between growing and melting ice nuclei, we distinguish these data points using different colors (blue and red, respectively) in the figures. It can be seen that even some large ice crystal nuclei with water molecule numbers greater than 800 are subject to melting. This is particularly evident for I_h which we will

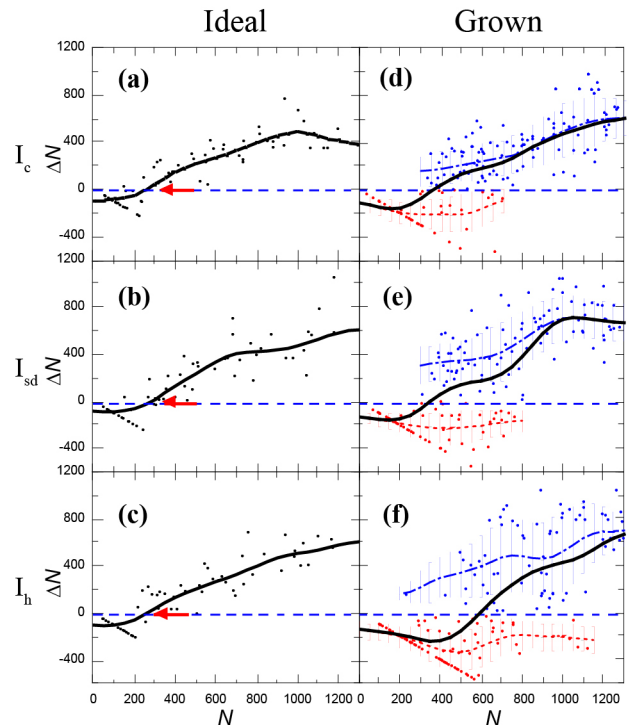


FIG. 2. Size changes ΔN of different ice polymorphs at the end of the “seeding” simulations versus their initial sizes N . From top to bottom are Ice I_c , Ice I_{sd} and Ice I_h , respectively. The black line represents the average size change for each cluster size. The blue dashed line marks $\Delta N = 0$, i.e. the growing-melting equilibrium line. (Left): Ideal ice nuclei. The blue dashed line and red arrow indicate the location of the critical nucleus size N_c . (Right): Spontaneously grown ice nuclei. The growing and melting data points are distinguished by blue and red colors, respectively. The blue dash dot lines and red dot lines represent the average size changes of growing and melting ice clusters, respectively.

discuss later with respect to Ostwald’s step rule. In contrast, a number of small ice crystal nuclei with only about 200 water molecules do grow. In such a situation, if one uses the $\Delta N = 0$ criteria for CNT to calculate the critical nucleus size, the error will be substantial, yielding an N_c ranging from 200 to 800 (see Table S2 in SI). This observation is in line with the vast variations in critical nucleus sizes obtained in different studies.

In contrast to ideal ice nuclei, the kinetics of spontaneously grown ice nuclei with varying polymorphisms exhibit notable differences. We computed several kinetics-related properties for these nuclei based on the CNT[20, 23] (See Chapter-S(VII) in the supplementary material), as summarized in Table I. Notably, the critical nucleation size N_c of ice I_{sd} is 351, a value closely aligns with thermodynamic calculations[15]. Our calculation results reveal that the growth rates of different polymorphic ice nuclei follow the order: Ice $I_{sd} \approx$ Ice $I_c >$ Ice I_h . However, from a thermodynamic perspective[16], their stabil-

ity ranking order is Ice I_{sd} > Ice I_h > Ice I_c . To understand this discrepancy, we performed MD simulations for each of the three distinct polymorphic ice nuclei, extending the simulations up to 3 μ s. Remarkably, after 2 μ s of simulation, all three systems—comprising 23,040 water molecules each—essentially completely froze, eventually converging into a mixed Ice I_{sd} state. (see Movie S1-3 and Chapter-S(VIII)). This observation reaffirms the thermodynamic stability of ice I_{sd} .

We speculate that the difference between spontaneously grown and ideal ice nuclei is related to the defects present in the former but not the latter. Since the ideal nuclei are defect-free spherical nuclei cut from perfect ice crystals, they grow isotropically. In contrast, spontaneously grown nuclei are characterized by a variety of defect structures, such as 5-8 water ring[32], five-fold twin boundaries[19], and predominant stacking in more than one direction[24]. These defects are expected to affect the kinetics of nuclei growth, causing them to differ from the ideal nuclei.

We first examined the surface defects of ice nuclei. Since different from the ideal nuclei, the grown nuclei are most likely not perfectly spherical, their surface area thus differ from that of the ideal nuclei with the same cluster size. We used the solvent accessible surface areas (SASA) S to denote the surface area of the nucleus and found that the ideal nucleus indeed has the smallest surface area for the same number of cluster particles, which is essentially proportional to $N^{2/3}$ (see Chapter-S(IX) in Supplementary Material). In contrast, spontaneously growing nuclei tend to have a larger surface area, suggesting a complex surface morphology. However, the surface area alone was shown unable to distinguish whether the nuclei will eventually grow or melt. FIG. 3(a) illustrates the relationship between ΔN and S , demonstrating that the final fate of spontaneously growing nuclei can be very different even when they have the same surface areas.

We next investigated the impact of internal defects of ice clusters on nucleation kinetics. We focused on the orientational order parameter q [15, 33, 34], a metric for assessing ice nucleus defects. Specifically, q characterizes tetrahedral configurations and reflects the lattice perfec-

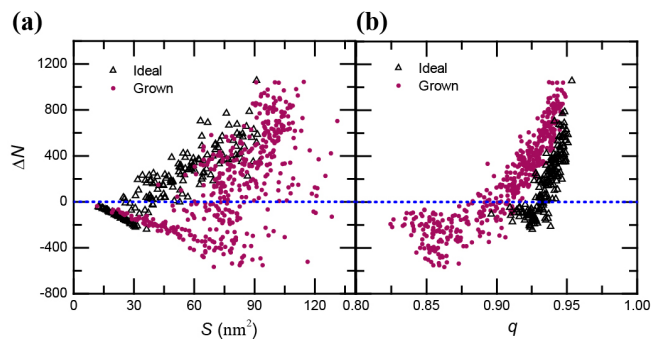


FIG. 3. Influence of internal and external defects in ice clusters on nucleation kinetics. Hollow black triangles indicate ideal ice nuclei and solid purple circles indicate spontaneously grown ice nuclei. The blue dashed line marks the position where $\Delta N = 0$. Plot of (a) ice cluster size changes ΔN versus solvent accessible surface areas (S), (b) Ice cluster size changes ΔN versus orientation order parameter q .

tion of crystals with a coordination number of four, such as ice[15]:

$$q = 1 - \frac{3}{8} \sum_{\alpha > \beta} \left(\cos \theta_{\alpha\beta} + \frac{1}{3} \right)^2, \quad (3)$$

where $\theta_{\alpha\beta}$ represents the angle formed by the lines connecting the oxygen atom of a given water molecule to those of its 4 nearest neighbors, denoted as α and β . FIG. 3(b) demonstrates a strong positive correlation between ΔN and q for both ideal ice nuclei and spontaneously grown ice nuclei. Furthermore, this parameter effectively distinguishes the growth behaviors of the two ice nucleus types, suggesting that q serves as a valuable indicator for ice nucleus kinetics.

Consequently, incorporating the orientation order parameter q alongside the nucleus size N as reaction coordinates provides a more comprehensive description of ice nucleation kinetics (see FIG. 4(a)). To visualize ice nucleus growth or melting more distinctly in a 2D representation, we employ a normalized relative ratio S_N of the size change ΔN , indicated by different colors for each data point (see Chapter-S(VI) in the Supplementary Material for details). Notably, FIG. 4(a) reveals a discernible boundary between growing and melting ice nuclei, which applies to both ideal and spontaneously grown nuclei. However, the impact of q on ideal ice nuclei is negligible, given their minimal variation (all exhibiting large values). In contrast, for spontaneously grown ice nuclei, the order parameter q is of similar importance as the nucleus size N in influencing kinetics. Even when the ice nucleus size N is large, it can eventually melt if the order parameter q is small—indicating a high prevalence of internal defects. Thus, the directional order parameter q , characterizing these internal defects, serves as an effective complement to the CNT approach, providing one more dimension for our understanding of natural ice nucleation kinetics.

The orientation order parameter q can also serve as

TABLE I. Theoretical estimated nucleation rate

	I_c	I_{sd}	I_h	I_{sd}^a
N_c	362	351	599	314
f^+ (/s)	4.24E+11	6.32E+11	7.69E+11	1.9E+11
Z	0.00705	0.00716	0.00548	0.0076
γ	70.33	69.61	83.19	67.0
$\Delta G(k_B T)$	61.41	59.55	101.62	52.8
$\log_{10}(J/m^3/s)$	11.00	11.99	-6.31	14.8

^a Ref. [15]

^b The supercooling temperature $\Delta T = 40$ K, $\Delta\mu = 0.155$ kcal/mol, as Ref. [15]. f^+ is the attachment rate of particles to the critical cluster. Z is the Zeldovich factor. γ is liquid–solid surface free energy. ΔG_c is nucleation free-energy barrier height. J is the nucleation rate.

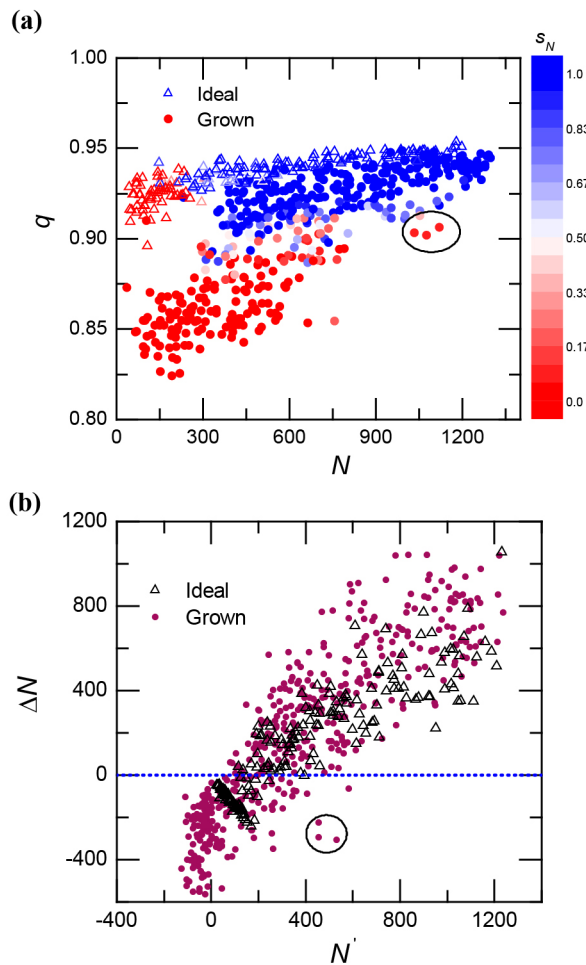


FIG. 4. The crystallization kinetics versus various cluster descriptors. Hollow triangles indicate ideal ice nuclei and solid circles indicate spontaneously grown ice nuclei. The black circle marks anomalous data points. (a) Scatter plot of the normalized relative ratios of size changes S_N as a function of the ice nucleus size N and the orientation order parameter q . Data points are color mapped by the value of S_N , with blue representing growth and red melting. (b) Size changes ΔN of ice nuclei versus “corrected” effective nuclei sizes N' . The blue dotted line marks the position where $\Delta N = 0$.

a correction factor for the ice nucleus size N , making it compatible with the conventional CNT approach. Here, we propose an effective ice nucleus size N' that is “corrected” by the following relation:

$$N' = N(1 - M(q_{max} - q)), \quad (4)$$

where M represents the second-order neighbor number of the crystal structure, and q_{max} is the fitting coefficient for ideal nuclei. For ice nuclei, we have $M = 12$ and $q_{max} = 0.95$. The relationship between the “corrected” effective ice nucleus sizes N' and the size changes ΔN is depicted in FIG. 4(b). Notably, both ideal and spontaneously grown ice crystal nuclei exhibit a strong positive

correlation with the effective size N' concerning their size change ΔN . Furthermore, there is no significant difference in the kinetic behaviors between the two types of ice nuclei when they are described using the effective size N' . (See Chapter-S(IX) in the supplementary material). Specifically, the data points for spontaneously grown ice nuclei at $\Delta N = 0$ are no longer as scattered as shown in FIG. 2(d-f). We have determined N'_c values for different polymorphic ice nuclei, which fall within a narrow range of 187 to 192.

However, we do observe three anomalous data points in FIG. 4(a). These data points correspond to large nucleus sizes N , and their order parameter q values are also relatively large. However, their size changes ΔN are negative. These three points show a behavior quite distinct from the other data points in the effective nucleus size N' illustrated in FIG. 4(b). Upon examining the structure of these three ice clusters, we discovered that they exhibit poly-crystalline characteristics. Specifically, their main bodies consist of I_h crystal structures coexisting with I_c fragments. During the “seeding” process, the coexisting I_c fragments rapidly dissolved or melted. Consequently, by the end of the 100 ns molecular MD simulation, the total number of molecules in the cluster showed a decrease from its initial value. However, the remaining portions of these ice clusters continued to grow slowly, as evidenced by our extension of the MD simulations for these three ice nuclei over a longer time (see Chapter-S(X) in the supplementary material). After examining the initial crystal structures of all other ice nuclei, we confirmed that only these three I_h ice nuclei exhibit such distinct poly-crystalline features. This observation suggests that these three cases are indeed special occurrences. However, it raises an intriguing question: Why only do the I_h ice nuclei have fragments of other crystals adhering to them? The answer might lie in the Ostwald’s step rule. Since ice I_c is kinetically faster to form than ice I_h , I_c fragments may grow on the surface of the slowly growing I_h ice clusters. However, ice I_h is thermodynamically more stable, so these I_c fragments can also rapidly melt, leaving the main body of the I_h nuclei to continue to grow. In another study[35], we found that 2-D ice clusters are also subject to a similar process of partial melting before freezing. Further studies are needed to shed more light into this process.

In summary, we propose here a generalized nucleation theory that describes satisfactorily the kinetics of ice nucleus growth in general conditions. Using all-atom MD simulations, we find that the ice formation from spontaneously grown ice nuclei deviates substantially from the classical nucleation theory, primarily due to defects existing in the ice nuclei. We then proposed to correct the CNT by incorporating the orientation order parameter q as a descriptor of these defects. The kinetics of ice nuclei in various states becomes well described with this simple correction. This result shows that defects within the nucleus are crucial and must be considered in studies of nucleation kinetics. The approach proposed in this letter

can also be applied to the kinetics study of other tetra-coordinated crystalline materials. For other types of crystals, alternative descriptors that characterize internal defects, such as Q_3 [19, 24, 36], Q_4 [20], Q_6 [19, 20, 23, 24, 37], can be used. We believe that this generalized nucleation theory has broad theoretical implications for nucleation kinetics and can inspire the study of various biochemistry and material systems[38–40].

The authors thank Haiyang Niu, Xueguang Shao,

Wensheng Cai, Haohao Fu, Mingyi Chen, Haipeng Wang for useful discussion. Computational resources were supported by Shenzhen Bay Laboratory supercomputing center. This research was supported by the National Science and Technology Major Project (No. 2022ZD0115003), the National Natural Science Foundation of China (22273061, 22003042 to Y.I.Y., and 21927901, 21821004, 92053202, 22050003 to Y.Q.G.) and the National Key Research and Development Program of China (2017YFA0204702 to Y.Q.G.).

-
- [1] L. del Rosso, M. Celli, F. Grazzi, M. Catti, T. C. Hansen, A. D. Fortes, and L. Ulivi, Cubic ice ic without stacking defects obtained from ice xvii, *Nature materials* **19**, 663 (2020).
- [2] T. Bartels-Rausch, V. Bergeron, J. H. E. Cartwright, R. Escribano, J. L. Finney, H. Grothe, P. J. Gutiérrez, J. Haapala, W. F. Kuhs, J. B. C. Pettersson, S. D. Price, C. I. Sainz-Díaz, D. J. Stokes, G. Strazzulla, E. S. Thomson, H. Trinks, and N. Uras-Aytemiz, Ice structures, patterns, and processes: A view across the icefields, *Rev. Mod. Phys.* **84**, 885 (2012).
- [3] D. Quigley, Communication: Thermodynamics of stacking disorder in ice nuclei, *The Journal of Chemical Physics* **141**, 121101 (2014).
- [4] B. J. Murray, D. A. Knopf, and A. K. Bertram, The formation of cubic ice under conditions relevant to earth’s atmosphere, *Nature* **434**, 2005 (2005).
- [5] A. Reinhardt and J. P. K. Doye, Free energy landscapes for homogeneous nucleation of ice for a monatomic water model, *The Journal of Chemical Physics* **136**, 054501 (2012).
- [6] H. König, Eine kubische eismodifikation, *Zeitschrift für Kristallographie - Crystalline Materials* **105**, 279 (1943).
- [7] J. M. Baker, J. C. Dore, and P. Behrens, Nucleation of ice in confined geometry, *The Journal of Physical Chemistry B* **101**, 6226 (1997).
- [8] A. Falenty and W. F. Kuhs, “self-preservation” of CO_2 gas hydrates—surface microstructure and ice perfection, *The Journal of Physical Chemistry B* **113**, 15975 (2009).
- [9] J. A. Sellberg, C. Huang, T. A. McQueen, N. D. Loh, H. Laksmono, D. Schlessinger, R. G. Sierra, D. Nordlund, C. Y. Hampton, D. Starodub, D. P. DePonte, M. Beye, C. Chen, A. V. Martin, A. Barty, K. T. Wikfeldt, T. M. Weiss, C. Caronna, J. Feldkamp, L. B. Skinner, M. M. Seibert, M. Messerschmidt, G. J. Williams, S. Boutet, L. G. M. Pettersson, M. J. Bogan, and A. Nilsson, Ultrafast x-ray probing of water structure below the homogeneous ice nucleation temperature, *Nature* **510**, 2014 (2014).
- [10] S. Pipolo, M. Salanne, G. Ferlat, S. Klotz, A. M. Saitta, and F. Pietrucci, Navigating at will on the water phase diagram, *Phys. Rev. Lett.* **119**, 245701 (2017).
- [11] A. Haji-Akbari and P. G. Debenedetti, Direct calculation of ice homogeneous nucleation rate for a molecular model of water, *Proceedings of the National Academy of Sciences* **112**, 10582 (2015).
- [12] A. J. Amaya, H. Pathak, V. P. Modak, H. Laksmono, N. D. Loh, J. A. Sellberg, R. G. Sierra, T. A. McQueen, M. J. Hayes, G. J. Williams, M. Messerschmidt, S. Boutet, M. J. Bogan, A. Nilsson, C. A. Stan, and B. E. Wyslouzil, How cubic can ice be?, *The Journal of Physical Chemistry Letters* **8**, 3216 (2017).
- [13] W. F. Kuhs, C. Sippel, A. Falenty, and T. C. Hansen, Extent and relevance of stacking disorder in ice ic, *Proceedings of the National Academy of Sciences* **109**, 21259 (2012).
- [14] Y. I. Yang, Q. Shao, J. Zhang, L. Yang, and Y. Q. Gao, Enhanced sampling in molecular dynamics, *The Journal of Chemical Physics* **151**, 070902 (2019).
- [15] H. Niu, Y. I. Yang, and M. Parrinello, Temperature dependence of homogeneous nucleation in ice, *Phys. Rev. Lett.* **122**, 245501 (2019).
- [16] M. Li, J. Zhang, H. Niu, Y.-K. Lei, X. Han, L. Yang, Z. Ye, Y. I. Yang, and Y. Q. Gao, Phase transition between crystalline variants of ordinary ice, *The Journal of Physical Chemistry Letters* **13**, 8601 (2022).
- [17] W. Ostwald, Studien über die bildung und umwandlung fester körper, *Zeitschrift für Physikalische Chemie* **22U**, 289 (1897).
- [18] B. J. Murray, S. L. Broadley, T. W. Wilson, S. J. Bull, R. H. Wills, H. K. Christenson, and E. J. Murray, Kinetics of the homogeneous freezing of water, *Phys. Chem. Chem. Phys.* **12**, 10380 (2010).
- [19] T. Li, D. Donadio, G. Russo, and G. Galli, Homogeneous ice nucleation from supercooled water, *Phys. Chem. Chem. Phys.* **13**, 19807 (2011).
- [20] E. Sanz, C. Vega, J. R. Espinosa, R. Caballero-Bernal, J. L. F. Abascal, and C. Valeriani, Homogeneous ice nucleation at moderate supercooling from molecular simulation, *Journal of the American Chemical Society* **135**, 15008 (2013).
- [21] J. R. Espinosa, A. Zaragoza, P. Rosales-Pelaez, C. Navarro, C. Valeriani, C. Vega, and E. Sanz, Interfacial free energy as the key to the pressure-induced deceleration of ice nucleation, *Phys. Rev. Lett.* **117**, 135702 (2016).
- [22] I. Sanchez-Burgos, A. R. Tejedor, C. Vega, M. M. Conde, E. Sanz, J. Ramirez, and J. R. Espinosa, Homogeneous ice nucleation rates for mW and TIP4P/ICE models through Lattice Mold calculations, *The Journal of Chemical Physics* **157**, 094503 (2022).
- [23] J. R. Espinosa, E. Sanz, C. Valeriani, and C. Vega, Homogeneous ice nucleation evaluated for several water models, *The Journal of Chemical Physics* **141**, 18C529 (2014).
- [24] L. Lupi, A. Hudait, B. Peters, M. Grünwald, R. G. Mullen, A. H. Nguyen, and V. Molinero, Role of stacking disorder in ice nucleation, *Nature* **551**, 218 (2017).
- [25] J. R. Espinosa, C. Navarro, E. Sanz, C. Valeriani, and

- C. Vega, On the time required to freeze water, *The Journal of Chemical Physics* **145**, 211922 (2016).
- [26] A. Laio and M. Parrinello, Escaping free-energy minima, *Proceedings of the National Academy of Sciences* **99**, 12562 (2002).
- [27] Y. Q. Gao, An integrate-over-temperature approach for enhanced sampling, *The Journal of Chemical Physics* **128**, 064105 (2008).
- [28] Y. I. Yang, H. Niu, and M. Parrinello, Combining metadynamics and integrated tempering sampling, *The Journal of Physical Chemistry Letters* **9**, 6426 (2018).
- [29] R. J. Allen, D. Frenkel, and P. R. ten Wolde, Simulating rare events in equilibrium or nonequilibrium stochastic systems, *The Journal of Chemical Physics* **124**, 024102 (2006).
- [30] X.-M. Bai and M. Li, Test of classical nucleation theory via molecular-dynamics simulation, *The Journal of Chemical Physics* **122**, 224510 (2005).
- [31] Y.-P. Huang, Y. Xia, L. Yang, J. Wei, Y. I. Yang, and Y. Q. Gao, Sponge: A gpu-accelerated molecular dynamics package with enhanced sampling and ai-driven algorithms, *Chinese Journal of Chemistry* **40**, 160 (2022).
- [32] P. Pirzadeh and P. G. Kusalik, On understanding stacking fault formation in ice, *Journal of the American Chemical Society* **133**, 704 (2011).
- [33] P.-L. Chau and A. J. Hardwick, A new order parameter for tetrahedral configurations, *Molecular Physics* **93**, 511 (1998).
- [34] J. R. Errington and P. G. Debenedetti, Relationship between structural order and the anomalies of liquid water, *Nature* **409**, 318 (2001).
- [35] Y. Zhao and Y. Q. Gao, Different intermediate water cluster with distinct nucleation dynamics among mono layer ice nucleation (2024), arXiv:2403.17544 [physics.chem-ph].
- [36] A. Hudait, D. R. Moberg, Y. Qiu, N. Odendahl, F. Paesani, and V. Molinero, Preordering of water is not needed for ice recognition by hyperactive antifreeze proteins, *Proceedings of the National Academy of Sciences* **115**, 8266 (2018).
- [37] P. M. Naullage, A. K. Metya, and V. Molinero, Computationally efficient approach for the identification of ice-binding surfaces and how they bind ice, *The Journal of Chemical Physics* **153**, 174106 (2020).
- [38] H. Niu, L. Bonati, P. M. Piaggi, and M. Parrinello, Ab initio phase diagram and nucleation of gallium, *Nature Communications* **11**, 2654 (2020).
- [39] H. Niu, P. M. Piaggi, M. Invernizzi, and M. Parrinello, Molecular dynamics simulations of liquid silica crystallization, *Proceedings of the National Academy of Sciences* **115**, 5348 (2018).
- [40] A. Hudait, N. Odendahl, Y. Qiu, F. Paesani, and V. Molinero, Ice-nucleating and antifreeze proteins recognize ice through a diversity of anchored clathrate and ice-like motifs, *Journal of the American Chemical Society* **140**, 4905 (2018).